ELSEVIER

Journal of Nuclear Materials 241-243 (1997) 1002-1007

journal of nuclear materials

Role of energetic particles in heat and particle exhaust in a poloidal divertor RFP

S. Masamune *, M. Iida, N. Oda, M. Awazu, K. Fujitsuka, K. Ohta, H. Oshiyama

Department of Electronics and Information Science, Kyoto Institute of Technology, Matsugasaki, Sakyo-ku, Kyoto 606, Japan

Abstract

In a closed poloidal divertor experiment in the STE-2 reversed field pinch (RFP), heat and particle exhaust into the RFP divertor region has been demonstrated. The exhaust efficiency, however, was lower than expected from equilibrium flux surface geometry near the divertor throat. In addition, indications of enhanced plasma-wall interaction (PWI) have also been observed. Particle orbit calculations have been carried out in the poloidal divertor configuration, showing that the complicated orbits depend strongly upon the particle energy, pitch angle and initial position. It has been concluded that energetic particles such as edge superthermal electrons or anomalously heated ions, both of which are common to the RFP, possibly enhance PWI near the divertor throat due to the effect of large Larmor radii, and reduce the exhaust efficiency also. It has also been shown that the orbits are quite sensitive to the initial positions near the separatrix, indicating the importance of edge magnetic fluctuations to the divertor action. Issues for future RFP divertor studies are also discussed.

Keywords: Poloidal divertor; Reversed field pinch; Fast particle losses; Particle balance

1. Introduction

The reversed field pinch (RFP) reactor concept is characterized by compactness, high beta and high power density [1]. Because of its high power density, the most crucial technological issue in the RFP is the control of plasma-wall interaction (PWI). Divertor studies, therefore, are of great importance for the development of RFP fusion reactor. The RFP divertor configurations have recently been achieved both in the closed [2,3] and open [4,5] configurations without appreciable influence on MHD activities. A closed poloidal divertor configuration was first achieved in the STE-2 with the use of a specific chamber [2]. Following non-observation of unfavorable MHD behavior in the RFP divertor configuration, behavior of the edge superthermal (fast) electrons in diverted RFP plasmas was studied, and the poloidal divertor capability of heat flux control has been demonstrated [3]. In an open poloidal divertor experiment in TPE-2M device [4], it was demonstrated that heat flux was localized along the magnetic separatrix, which caused early current termination due to an increase in impurity influx. In TPE-2M, an open RFP toroidal divertor configuration [5] has also been achieved, showing some favorable influence and interesting features.

In the present paper, particle and impurity behaviors in the closed poloidal divertor configuration in STE-2 are discussed. It is demonstrated that some part of the particle flux was exhausted into the RFP divertor region. The exhaust efficiency was, however, lower than expected from equilibrium flux surface geometry. In addition, some indications about enhanced PWI were observed, as a result of the divertor application. Particle orbit calculations in the poloidal divertor RFP have been carried out, showing that such unfavorable influence can be attributable, at least partly, to the energetic particles such as edge superthermal electrons and anomalously heated ions. Issues for optimization of the poloidal divertor configurations will also be discussed.

2. Experimental results

Experiments were performed in the STE-2 RFP, which used a 2 mm thick SS main chamber of 40 cm major

* Corresponding author. Tel.: +81-75 724 7420; fax: +81-75 724 7400; e-mail: masamune@dj.kit.ac.jp.

PII S0022-3115(96)00648-4

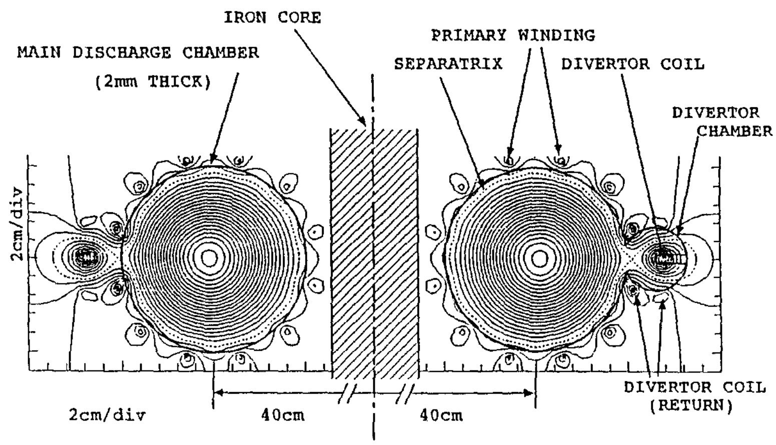

Fig. 1. A false cross-sectional view of the discharge chamber with the left-hand side showing the gap region cross section and the right-hand side far from the gap.

radius (R_0) and 10 cm minor radius (a), and an outer divertor chamber. The main chamber was covered by a 0.5 mm thick copper shell. The primary windings were set coaxially with the main plasma column, distributing around the main chamber. The details are described in Refs. [2,3]. The main chamber had two 5 mm wide poloidal gaps, each of which was insulated by a ceramic insulator. The outer divertor chamber also had two 7 cm wide gaps, where the magnetic field lines were intercepted by SS plates, at the poloidal gap flanges of the main chamber. A cross sectional view is given in Fig. 1, together with contours of the poloidal flux function obtained from the equilibrium analysis with the divertor to plasma current ratio of 20%.

Radial profiles of the ion saturation current were measured with electrostatic double probes both in the divertor region and at the main plasma edge ($0.8 \leq r/a \leq 1.0$). The probe electrodes were 3 mm long and 0.3 mm in diameter, being separated by 3 mm from each other. They were shielded by a ceramic tube of 10 mm inner diameter in order to minimize the effect of the superthermal electrons. This shield makes it difficult to estimate the plasma density accurately from the ion saturation current. Therefore, the following discussion on the plasma particle behavior is based on the ion saturation current rather than ion density. In addition to the probes, recycling neutral particles and impurity behavior were studied with two single-chord visible light spectrometers.

Fig. 2 shows time evolution of the radial profiles of the ion saturation current 1 cm above the midplane in the divertor region ($R \geq 50$ cm, where the poloidal null is located at $R \sim 50.5$ cm), together with time traces of the plasma and divertor currents. The divertor current was turned on 0.2 ms into the discharge. It took about 0.1 ms for the applied field to penetrate the chamber to form a closed divertor configuration. Thus, in the present experiments, closed poloidal divertor configurations were sustained for 0.3–0.4 ms. After setting up of the divertor configuration (0.50 ms), the ion saturation current increased by a factor of 2 to 10 well inside the divertor region, maintaining the profile for the rest of the discharge.

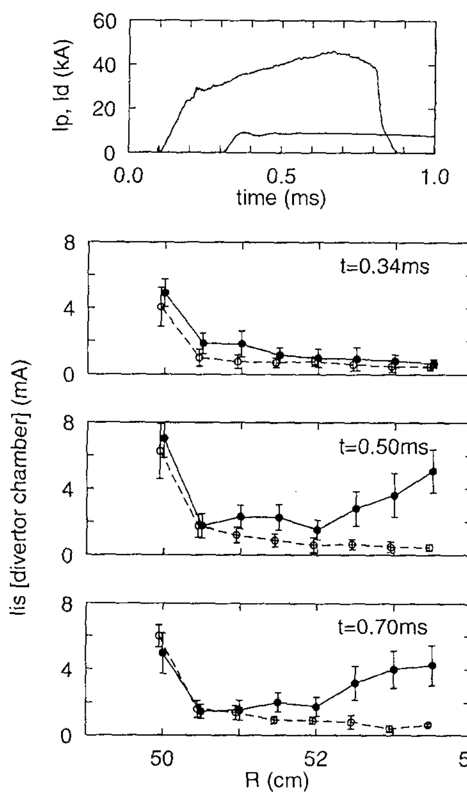

Fig. 2. Time evolution of the radial profiles of the ion saturation current in the divertor region 1 cm above the midplane. The solid (dashed) line is for diverted (undiverted) discharge. In diverted discharges, the poloidal rull is located at $R = 50.0$ cm. Time trace of the plasma and divertor currents is given at the top, in which the divertor current is turned on 0.2 ms into the discharge.

H_α line intensity also increased in the divertor region by a factor of 2 to 3. This is a demonstration that plasma particles are exhausted into the divertor region in a closed RFP poloidal divertor. The incremental saturation current is almost equal to that at the extreme plasma edge ($R = 50$ cm), which is lower than expected from the equilibrium flux surface geometry, if the outward particle flux across the magnetic separatrix is converted to a parallel flux which is then exhausted into the divertor region along the magnetic separatrix.

Fig. 3 shows time traces of the impurity line intensities in both the main and diverted plasmas. In the diverted plasma line intensities of both the oxygen (low Z) and chromium (metal) impurities increased by a factor of 2 to 3 when the divertor field was applied. It should also be noted that the chromium line intensity increased in the main plasma region also as a result of the divertor application. The oxygen line might also increase slightly. Other spectroscopic and probe results are summarized as follows: H_α line intensity in the main plasma increased by a factor of 1.5 to 2, and the edge ion saturation current (corresponding to density) increased also by a factor of 1.5 to 2, when the divertor field was applied. These results indicate that some part of the particle flux can be exhausted into the RFP divertor region. And, at the same time, PWI in the main plasma is enhanced, which gives rise to the increased impurity line intensities and enhanced recycling neutrals at the main plasma edge in diverted RFP discharges.

This should be compared with the heat flux studies discussed in Ref. [3]. The field aligned high heat flux both at the main plasma edge (~ 100 MW/m^2) and in the divertor region (~ 20 MW/m^2) was carried mainly by the superthermal (with 'temperature' about ten times the central value) electrons [6]. Larmor radii of these energetic electrons are not negligible compared with the clearance between the separatrix and the wall or the divertor throat width. Therefore, the energetic electrons will have influence on the heat exhaust efficiency.

The ion energy may also be important, because the anomalous ion heating is a universal phenomenon in the RFP [7], which usually results in the ion temperature almost equal to the electron temperature. If it applies to the main plasma edge in the STE-2, Larmor diameter of the thermal ion ($T_i \sim 10$ eV) can be larger than the divertor throat width. Thus, the anomalously heated thermal ions will have influence on the PWI, particle recycling and particle exhaust efficiency.

3. Particle orbit calculations

In order to obtain an idea about the influence of energy and pitch angle of the plasma particles on heat and particle exhaust, particle orbit calculations were performed in a cylindrical plasma with the STE-2 geometry. For the purpose of simplicity, filament current approximation was used in the poloidal field due to the primary current, plasma current, divertor and return currents. It is a good approximation for the poloidal field near the plasma edge. The Bessel function profile was used for the toroidal magnetic field (field reversal surface at $r/a = 0.86$) in the region $r/a \leq 0.95$, outside of which uniform distribution was assumed. Toroidicity in the magnetic field was taken into account. Other parameters for the calculation were as follows: plasma current of 48 kA, divertor current of 10 kA, and inductive toroidal electric field of 100 V/m.

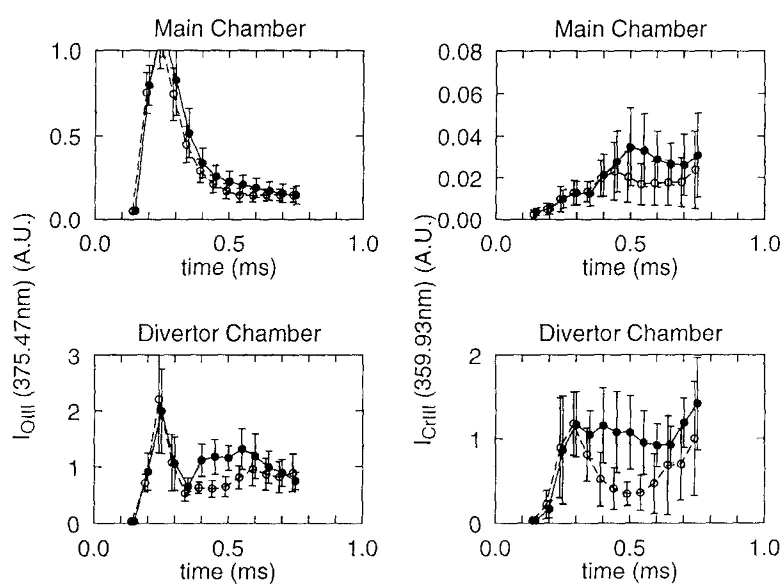

Fig. 3. Time traces of the impurity line intensities in both the main and diverted plasmas. The solid (dashed) line is for diverted (undiverted) discharge.

Ambipolar electric field was out of the scope of the present calculation.

Particle orbit was calculated in a (x, y, z) coordinate system with poloidal cross section in the (x, y) plane and the z-axis in the toroidal direction. The origin was taken at the center of the torus. The calculation started from an initial position until the particle was eventually diverted or hit the main chamber wall, for specific values of the initial energy and pitch angle. Some examples of the proton orbits in the (x, y) plane are given in Fig. 4. In Fig. 4(a), a proton with an initial energy of 4 eV and pitch angle of 10° starts from the initial position (0.400, 0.088) (unit: m). This proton is eventually diverted. In Fig. 4(b), another example of the orbit is given of a proton with the same energy and pitch angle but from different initial position (0.320, 0.020). This proton eventually hit the edge of the divertor throat (undiverted). In both cases, the three dimensional orbit is very complicated.

An example of the results is summarized in Table 1. In the table, the ultimate position of a particle with a specific energy and a pitch angle is designated by D, M and Z, where D designates the divertor wall (diverted particle), M, the main chamber wall (undiverted particle) and Z, the SS plate at the insulated gap (diverted), respectively. Table 1a is the result of proton orbit calculations from the initial position (0.400, 0.086), which corresponds to slightly inside the separatrix above the minor axis. The table shows that most of the low energy particles and high energy particles with pitch angle near 90° hit the wall, while some of those with smaller pitch angles are diverted. This should be compared with Table 1b which is from the initial position (0.498, 0.004), slightly inside the separatrix near the poloidal null. This shows that high energy particles with pitch angles near 90° tend to hit the wall near the divertor throat. The same tendency was observed for the electron orbits. The results will provide the following picture.

In the STE-2, the primary windings were set close to

Table 1
Results of the ion orbit calculations for the initial positions of (a) (0.400, 0.086) and (b) (0.498, 0.004) in the (x, y) plane (unit in m) [a]

	Energy (eV)	Pitch angle (degree) 0.................45................90...............135...............180
(a)	0.05	M M M M M M M M M M M M M M M M M M M M M M M M M M M M M M M M M M M M M
	0.45	M M M M M M M M M M M M M M M M M M M M M M M M M M M M M M M M M M M M M
	1.25	M M M M M M M M M M M M M M M M M M M M M M M M M M M M M M M M M M M M M
	2.45	M D M D D D D M M M M M M M M M M M M M M M M M M M M M M M M M M M M M M
	4.05	M M M D M D D D D M M M M M M M M M M M M M M M M M M M M M M M M M M M M
	6.05	D D D M M M M M D D M M M M M M M M M M M M M M M M M M M M M M M M M M M
	8.45	M M M D D M M D M M M M M M M M M M M M M M M M M M M M M M D M D M D D D
	11.25	M M M D D M D M D D D M M M M M M M M M M M M M M M M D D D M D M D D D D
	14.45	D D D D D D M M D D D M M M M M M M M M M M M M M M M M D D M D D D D D D
	18.05	D D D D D D M M D D D M M M M M M M M M M M M M M M M M M D D D D D D D D
	22.05	D D M D M M D D D M D M M M M M M M M M M M M M M D M M D D D D D D D D D
	26.45	M M D M D D D M M M M M M M M M M M M M M M M M M M M M D D D D M D D D D
	31.25	M D D D D D M D D M M D M M M M M M M M M M M M M M D D D D D M D D D D D
	36.45	D D D D D D D D D M M M M M M M M M M M M M M M M M D M D D M D M D D D D
	42.05	M D D D D D D D D M M M D M M M M M M M M M M M M M M M D D D D D M D D D
(b)	0.05	D D D D D D D D D D D D D D D D D D D D D D D D M M M M M M M M M M M M M
	0.45	D D M M M M M M M D M M D M D D D D M D D D D D D D D D M M M M M M M M M
	1.25	M M D D M D D D D D M M D D M D M D D D D D D D D D D D M M M M M M M M M
	2.45	M M D D D D D M D D M D D M D M D M D D D M D M D D M D D M M M M M M M M
	4.05	D M M D D D M D D D D D M M D M D M M D D D D D M D M M M M M M M M M M M
	6.05	M M M D D D D D D M M M M M M M M D D D D D D M M D M M M M M M M M M M M
	8.45	D D M M D M M D M M M M M D M M M D D M M D D D M D M M M M M M M M M M M
	11.25	M D M M D M D M M M M M M M D D D M D D M D D D D M D M M M M M M M M M M
	14.45	D D D M D M D M M M M M M M M D D M D M M D D D D M D D M M M M M M M M M
	18.05	M D D M D M D M M M M M M M M M M D M D D M D D M M D M M M M M M M M M M
	22.05	M D M M D M M M M M M M M M M M M D M M D M D D D M D M M M M M M M M M M
	26.45	M D D M D D M M M M M M M M M M M M M D D D D D M M D M M M M M M M M M M
	31.25	D M D M D M M M M M M M M M M M M M M M D D D D M M D M M M M M M M M M M
	36.45	M D D M D D M M M M M M M M M M M M D M M D D D D M D M M M M M M M M M M
	42.05	D D D M D M M M M M M M M M M M M M D M M D M D D M D M M M M M M M M M M

[a] D and M indicate that the ion with specific initial energy and pitch angle eventually hit the divertor and the main chamber wall, respectively.

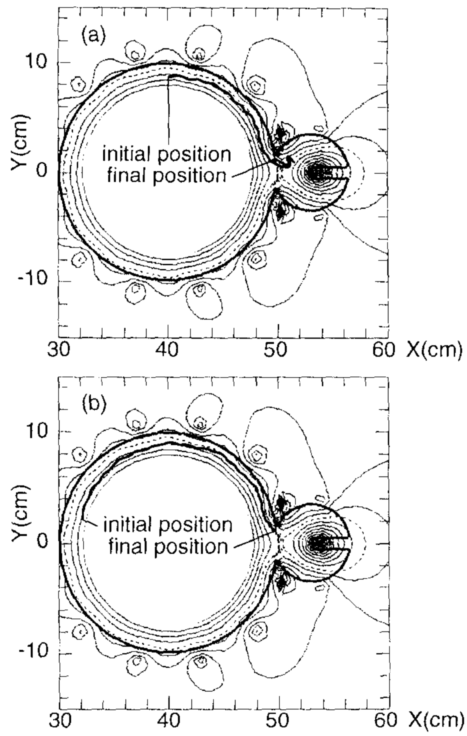

Fig. 4. Examples of the proton orbits together with contours of the flux function in the (x, y) plane. A proton with an initial energy of 4 eV and pitch angle 10° starts from the initial position of (a) (0.400, 0.088) and (b) (0.320, 0.020). In (a), the proton is diverted, while the proton hit the edge of the divertor throat in (b).

the plasma column for close coupling and fast current rise. In this configuration, poloidal field ripple (periodic change in the poloidal field intensity in the poloidal direction) near the edge ($|\Delta B_p|/B_p \sim 5\%$ (2%) at $r/a = 0.9(0.8)$) gives rise to trapped particles, having an influence on the particle velocity distribution function. The poloidally trapped particles, unless affected by collisions, eventually hit the wall. When the poloidal divertor is applied, pitch angle of the circulating particle is influenced near the poloidal null, where direction of the magnetic field line changes with a short scale length. The Larmor radius of the particle thus becomes large as a result of the combined effect of increased $v_\perp$ and decreased poloidal field intensity. Some of the particles are transferred from circulating to trapped particles. Those particles which hit the divertor throat will enhance the plasma–wall interaction locally, and, conversely, decrease the particle and heat exhaust efficiency.

It has also been found that the orbit is quite sensitive to the initial position near the separatrix, which applies particularly to electrons. For example, only 2 mm radial difference in the initial position causes a significant difference in the fraction of diverted electrons. This result indicates the importance of magnetic field fluctuations, which were neglected in the present orbit calculations. In the STE-2, fluctuation level of the edge radial field was of the order of 1%. This causes a radial fluctuation of the separatrix of the same level, far from the poloidal null. The fluctuational fraction of the separatrix near the poloidal null is much larger (~ 40%). Thus, the magnetic fluctuation has influence on the divertor action through sensitiveness of the orbit to the initial position. The magnetic field line stochasticity resulting from magnetic reconnection associated with MHD instabilities, often observed in the RFP core region in nonlinear MHD simulations, may not apply to the edge region [8].

4. Summary and discussion

Particle and impurity behaviors were studied in a closed poloidal divertor RFP. The results have shown that some part of the particle flux can be exhausted into the RFP divertor region. It has thus been demonstrated that the poloidal divertor is a possible means for heat and particle control in the RFP. And, at the same time, enhancement of PWI and recycling is observed when the divertor field is applied in the present configurations. Particle orbit calculations were carried out in the poloidal divertor configuration of the STE-2. The results have shown that relatively low efficiency of heat and particle exhaust and the enhanced PWI can be attributable, at least partly, to the energetic particles such as edge superthermal electrons end anomalously heated ions.

The physics issues for further studies on the poloidal divertor RFP can be summarized as follows. From the MHD point of view, the maximum permissible divertor scrape-off layer thickness, which has influence particularly on the stability of external ideal modes, has to be made clear. And, similarly, the maximum permissible divertor throat width, which may affect localized modes, or, localized disturbance, has to be made clear also. Both of these quantities determine the divertor efficiency geometrically.

The mechanism of the production of energetic particles such as superthermal electrons and anomalously heated ions has not been made clear yet. In any case, it is likely that the mechanism is closely related to the RFP dynamics, such as magnetic reconnection associated with nonlinear mode coupling. It is required to study the mechanism and to develop possible means for the control of the mechanism.

References

[1] H.A.B. Bodin and A.A. Newton, Nucl. Fusion 20 (1980) 1255.
[2] M. Iida, T. Miyagi, D. Ishijima et al., Plasma Phys. Controlled Fusion 36 (1994) 153.

[3] D. Ishijima, M. Iida, S. Masamune et al., Plasma Phys. Controlled Fusion 37 (1995) 657.
[4] K. Hattori, N. Hayase and Y. Sato, J. Phys. Soc. 63 (1994) 2177.
[5] K. Hattori, N. Hayase and Y. Sato, J. Phys. Soc. Jpn. 63 (1994) 1232.
[6] A. Mori, M. Iida S. Masamune et al., J. Phys. Soc. Jpn. 63 (1994) 3548.
[7] E. Scime, M. Cekic, D.J. Den Hartog et al., Phys. Fluids B 4 (1992) 4062.
[8] J.A. Holmes, B.A. Carreras, T.C. Hender et al., Phys. Fluids 28 (1985) 261.